J. Membrane Biol. 180, 123–136 (2001)
DOI: 10.1007/s002320010064

The Journal of
Membrane
Biology

ED_{50} G_{Na} Block Predictions for Phenyl Substituted and Unsubstituted *n*-Alkanols

A. Kondratiev*, R. Hahin
Department of Biological Sciences, Northern Illinois University, DeKalb, IL 60115, USA

Received: 11 August 2000/Revised: 21 December 2000

Abstract. To study the role the phenyl group plays in producing local anesthetic block, a sequence of *n*-alkanols and phenyl-substituted alkanols (Φ-alkanols) were characterized in their ability to block Na channels. The sequence of *n*-alkanols studied possess 3–5 carbons (propanol-pentanol). The action of phenol and 3-Φ-alkanols (benzyl alcohol, phenethyl alcohol, 3-phenyl-1-propanol) were also studied. Na currents (I_{Na}) were recorded from single frog skeletal muscle fibers using the Vaseline-gap voltage clamp technique. I_{Na}s were recorded prior to, during, and following the removal of the solutes in Ringer's solution.

All alkanols and phenol acted to block I_{Na} in a dose-dependent manner. Effective doses to produce half block (ED_{50}) of I_{Na} or Na conductance (G_{Na}) were obtained from dose-response relations for all solutes used. The block of G_{Na} depended on voltage, and could be separated into voltage-dependent and -independent components. Each solute acted to shift G_{Na}-V relations in a depolarized direction and reduce the maximum G_{Na} and slope of the relation. All solutes acted to speed up I_{Na} kinetics and cause hyperpolarizing shifts in steady-state inactivation. The magnitude of the kinetic changes increased with dose.

Size was an important variable in determining the magnitude of the changes in I_{Na}; however, size alone was not sufficient to predict the changes in I_{Na}. ED_{50}s for G_{Na} and AP block could be predicted as a function of intrinsic molar volume, hydrogen bond acceptor basicity (β) and donor acidity (α), and polarity (P) of the solutes.

The equivalency of ED_{50} predictions for AP and G_{Na} block can be explained by the fact that AP block arises from channel block and solute-induced changes in I_{Na} kinetics. Φ-alkanols were more effective at blocking and inactivating Na channels than their unsubstituted counterparts. Phenyl-substituted alkanols are more likely to interact with the channel than their unsubstituted counterparts.

Key words: Na current block — Na conductance block — Na kinetics — Alkanols — Phenyl substitution

Materials and Methods

The Vaseline-gap voltage-clamp method was used to record Na^+ currents (I_{Na}s) and characterize the kinetic and steady-state changes of I_{Na} caused by the application of test solutes to muscle fibers. A more complete description of the method is found in Larsen, Gasser & Hahin (1996). A brief description follows: single fibers were dissected from frog (*Rana pipiens*) semitendinosus muscles and voltage clamped using a modified version of the original Hille and Campbell (1976) Vaseline-gap voltage-clamp method. Improvements in the technique described previously (Campbell & Hahin, 1983) reduced the series resistance to a range of 0.5–1.5 Ωcm^2 and increased the fidelity of the recording of Na^+ currents. The improvements also virtually eliminated the contribution of transverse tubular (T) system current from the total current, thus allowing the surface Na^+ current to be solely recorded.

To speed up the removal of the T-system current from the total current (to isolate the surface current), a new procedure was employed and is described below: Instead of replacing CsF solution with standard Ringer's solution prior to each experiment, a high Ca^{2+} (20 mM) Ringer's solution was applied for 20–30 min followed by the application of Ringer's solution. This procedure caused a more rapid precipitation of Ca^{2+} in the T-tubules and acted to rapidly eliminate Na^+ and slow capacitive currents associated with the T-sysem.

Voltage-clamp command pulses were generated by a digital stimulator whose timing was controlled by a Digitimer D4030 (Medical Systems, Great Neck, NY). Subtraction of linear leakage currents was performed using an analog electronic transient generator. The subtracted current records were filtered using a 40 KHz filter. Current records were sampled at 10 μsec using a Nicolet 2090 digital oscilloscope (Nicolet Instrument, Madison, WI), and stored on minidiskettes for later analysis. The voltage-clamp, electronic leak subtractor, and the digital stimulator were built by R. Hahin.

* *Present address:* Department of Medicine, Division of Cardiology, The Johns Hopkins University School of Medicine, 720 North Rutland Ave., Ross 844, Baltimore, MD 21205, USA

Correspondence to: R. Hahin

The membrane potential was held at a holding potential of −140 mV to eliminate the effects of slow inactivation of Na^+ channels. Na^+ currents were elicited by 6 msec duration test pulses ranging in amplitude from −60 to +100 mV. Pulses were applied in steps of 10 mV with 6 sec intervals between pulses to insure full recovery from slow I_{Na} inactivation. All experiments were performed at 12°.

Protocol to Obtain Dose-Response Relations

To obtain dose-response relations, Na^+ currents were recorded in control Ringer's solution followed by successive applications of the test solutes and a return to Ringer's solution (if possible). Sequences of different concentrations of test solutes in Ringer's solution were applied externally to fibers typically in an ascending order from lower to higher concentration. For short chain *n*-alkanols the following procedure was used: a sequence of ascending doses was applied until full I_{Na} block was observed, followed by solute removal and recovery in Ringer's solution. In some experiments, a single dose of a test solute was applied followed by recovery.

Animals

Grass frogs (*Rana pipiens*) were purchased from Charles Sullivan, Nashville, TN. Animals were ethanized in accordance with procedures deemed acceptable by the Institutional Animal Care and Use Committee of Northern Illinois University.

Solutions

Ringer's solution contained (in mM): 112 NaCl, 2 KCl, 2 $CaCl_2$, and 10 HEPES. The high Ca^{2+} Ringers solution contained in mM: 85 NaCl, 2 KCl, 20 $CaCl_2$, and 10 HEPES. The internal solution contained (in mM): 115 CsF, 5 NaF, and 4 HEPES. All test solutions were prepared using a volume per volume dilution of test solutes in Ringer's solution. The solutes used were: ethanol, *n*-propanol, *n*-butanol, benzyl alcohol, phenethyl alcohol, 3-phenyl-1-propanol, and phenol. The pH of all solutions was adjusted to 7.4 with NaOH. *n*-Propanol, benzyl alcohol, phenethyl alcohol, 3-phenyl-1-propanol were purchased from Aldrich Chemical, Milwaukee, WI; methanol, ethanol, *n*-butanol, *n*-heptanol, *n*-hexanol, and phenol were purchased from Sigma Chemical, St. Louis, MO.

I_{Na} Data Analysis

The degree of I_{Na} block was defined to be the maximum I_{Na}, obtained from the *I-V* relation observed in the presence of the solute, divided by the maximum I_{Na} from the *I-V* relation, obtained in Ringer's solution prior to solute application. Maximum I_{Na} amplitudes were expressed as a fraction (relative maximum I_{Na}) of control values. Error bars represent the mean ± SEM. A 50% effective dose for I_{Na} block (ED_{50}) was defined to be the concentration of solute in Ringer's solution that produced a 50% reduction of the maximum I_{Na} amplitude. ED_{50}s were obtained from each dose-response relation. The potency of each test solute was defined as the reciprocal of its ED_{50} ($1/ED_{50}$). The relative potency (RP) of each solute was normalized so that methanol has a RP of 1. Statistical significance of differences in mean values was established at $P < 0.05$ by an unpaired *t*-test.

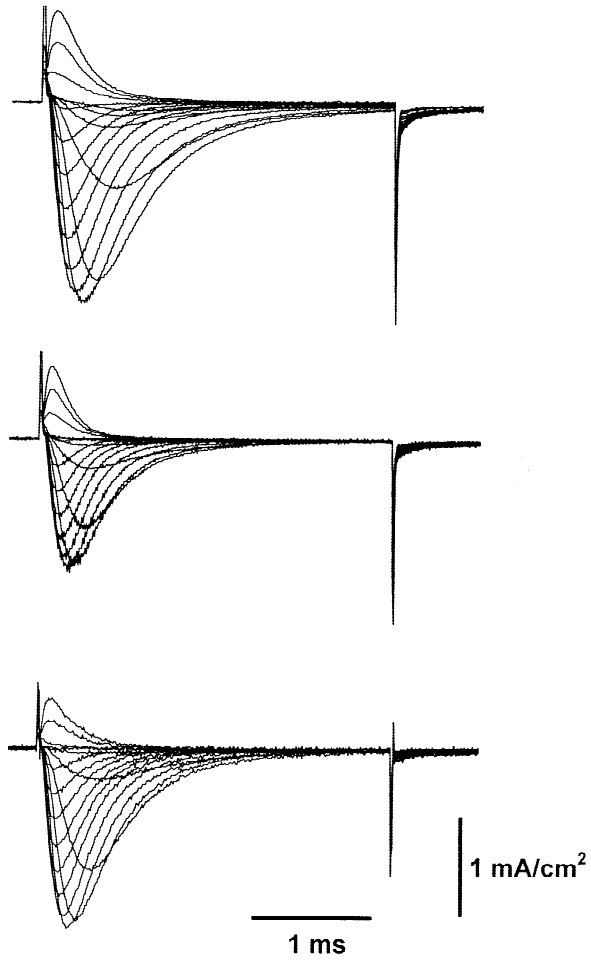

Fig. 1. Effect of *n*-pentanol on Na^+ currents. I_{Na} traces recorded at 16 voltages in Ringer's solution (upper panel), in the presence of 10 mM *n*-pentanol (middle panel) and after washout of pentanol with Ringer's solution. All currents were elicited using a test pulse of 6 msec duration from a holding potential of −140 mV. Test pulses were applied in steps of 10 mV from −60 to +100 mV at 12° C.

Results

Reversible Alkanol-Induced Block of Na^+ Currents

To characterize the effect of test solutes on I_{Na}, a sequence of I_{Na}s was elicited and recorded at 16 different membrane potentials in Ringer's solution, in the presence of test solutes, and upon recovery in Ringer's solution. Figure 1 illustrates a typical experiment. Figure 1 shows I_{Na}s recorded in Ringer's solution (top panel), in the presence of 15 mM *n*-pentanol (middle panel), and after washout in Ringer's solution (bottom panel). After return to Ringer's solution, recovery in this experiment was 90%; the average recovery for all solutes was 96 ± 2% ($n = 36$). Similar families of currents were observed

for all other test solutes. Na current-voltage (*I-V*) relations were constructed for all test solutes using records similar to that shown in Fig. 1.

Figure 2 shows *I-V* relations obtained for all test solutes at near half-blocking doses. The plotted symbols represent the peak I_{Na} amplitudes as a function of the test pulse potential. Each test solute *I-V* relation (filled circles) was superimposed upon the *I-V* relations obtained in Ringer's solution prior to (open circles) and after (open squares) application of a test solute. The *I-V*s recovered completely after the removal of each test solute. Following the removal of ethanol, recovery I_{Na}s exceeded their pre-application values. This effect was previously observed by Haydon and Urban (1986). *I-V* relations obtained in the presence of test solutes were also shifted to more positive potentials as the concentration of the test solutes increased. Upon recovery, the shifts in *I-V*s produced by test solutes disappeared.

Dose-Response Relations for I_{Na} and G_{Na} Block

Figure 3 represents dose-response relations plotted semilogarithmicaly and fit with solid traces for *n*-alkanols (open symbols) and Φ-alkanols (filled symbols). Also shown is the dose-response relation for phenol (filled diamonds) fitted with an interrupted trace. Each of the dose-response relations was fit by a logistics equation:

$$I_{Na(RA)} = \frac{1}{1 + \left(\frac{c}{ED_{50}}\right)^{b}} \quad (1)$$

where $I_{Na(RA)}$ is the maximum I_{Na} relative amplitude, *c* is the solute concentration in Ringer's solution, ED_{50} is the half-blocking dose, and *b* is the slope parameter. Best fit parameters for each logistics equation were obtained using a Marquardt-Levenberg nonlinear least square curve fitting algorithm. Figure 3 shows that increases in chain length cause a reduction in the ED_{50} which can be observed as a leftward shift of each dose-response relation for *n*-alkanols and Φ-alkanols.

These leftward shifts represent increases in potency caused by adding a methylene group to the carbon backbone of the molecule. The trace used to fit propanol (open triangles) can be shifted leftward and superposes well onto every other dose-response relation with increasing chain length; this shows that the slope for each relation is not significantly changed with an increase in chain length and the addition of a phenyl group. Since it was not possible to obtain *I-V*s in the presence of extremely large (>1 M) concentrations of ethanol, the dose-response relation for ethanol was incompletely described. Therefore, an average slope for all other *n*-alkanols was calculated and used to fit the dose-response relation for ethanol.

Table 1. ED_{50}s for I_{Na} block

Solute	I_{Na} block		
	ED_{50} mM	*b*	Log K_{ow}
n-Alkanols			
Methanol	1953*		−0.77
Ethanol	779 ± 128	1.71**	−0.31
Propanol	171 ± 11	1.78 ± 0.22	0.25
Butanol	70 ± 3	1.63 ± 0.16	0.88
Pentanol	16 ± 0.8	1.73 ± 0.23	1.56
Phenol and Φ-Alkanols			
Phenol	6.3 ± 0.4	1.86 ± 0.29	1.46
Benzyl alcohol	11.7 ± 0.3	1.84 ± 0.13	1.10
Phenethyl alcohol	6.7 ± 0.4	1.52 ± 0.18	1.51
3-Phenyl-1-propanol	2.7 ± 0.1	1.93 ± 0.19	2.05

ED_{50}–Effective Dose producing 50% block of I_{Na} and G_{Na}.
b–slope parameter used to fit equation:

$$I_{Na(RA)} = \frac{1}{1 + \left(\frac{c}{ED_{50}}\right)^{b}},$$

where *c* is a solute concentration.
*–ED_{50} for I_{Na} block was estimated from: $ED_{50} = 396/(K_{ow}^{0.90})$.
**–slope parameter is a calculated average for *n*-alkanols.

ED_{50}s for I_{Na} Block

Table 1 tabulates the experimentally obtained values of ED_{50} and Log K_{ow} obtained from the published results of Leahy et al. (1988) and el Tayar et al. (1991) for all test solutes used. Table 1 shows that the ED_{50} decreases as the chain length increases for *n*-alkanols and Φ-alkanols. Phenol is included for comparison purposes. As described in the previous section, the slope parameter (*b*) used in Eq. 1 to describe $I_{Na(RA)}$ was not significantly different for *n*-alkanols and Φ-alkanols. This suggests that increases in chain length produced potency increases that can be interpreted as simple shifts of a shape invariant dose-response relation.

G_{Na}-V Relations

I-V relations for the test solutes were converted to Na^+ conductance (G_{Na}) *vs.* voltage (G_{Na}-*V*) relations using the following equation:

$$G_{Na} = I_{Na}/(V_m - V_{Na}), \quad (2)$$

where I_{Na} is the current recorded at a membrane potential V_m and V_{Na} is a reversal potential obtained from each *I-V* relation.

Each G_{Na}-*V* relation was fit using Eq. 3 to determine the maximum G_{Na} ($G_{Na(max)}$) in Ringer's solution (control and recovery) and in the presence of each test solute:

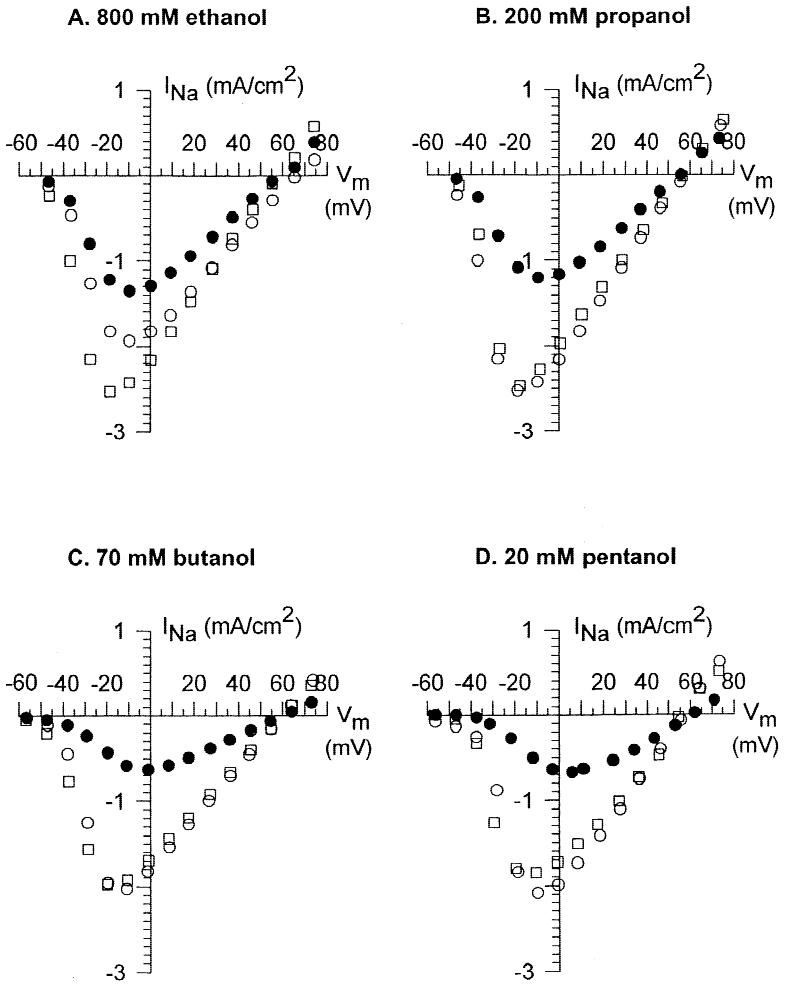

Fig. 2. (*A–D*) Na^+ current-voltage relations for solutes at near ED_{50} concentrations. *I–V* relations obtained from fibers bathed in Ringer's solution (open circles), in the test solute at near ED_{50} concentration (filled circles), and in Ringer's solution following washout of solute (open squares). The data points represent the peak Na^+ current plotted as a function of the test pulses superimposed on a holding potential of −140 mV. Each curve set represents one experiment at the concentration indicated for (*A*) ethanol, (*B*) *n*-propanol, (*C*) *n*-butanol, (*D*) *n*-pentanol.

$$G_{Na} = \frac{G_{Na(max)}}{1 + \exp\left(\frac{-zF(V_m - V_{1/2})}{RT}\right)}, \qquad (3)$$

where G_{Na} is the observed Na conductance at V_m, $G_{Na(max)}$ is the maximum Na conductance, $V_{1/2}$ is the membrane potential when conductance is reduced by 50%, z is the slope at the midpoint of G_{Na}-V relations, F is Faraday's constant, R is the gas constant, and T is the absolute temperature.

Differences in the shape of G_{Na}-V relations obtained in Ringer's solution and in the presence of a solute reveal whether Na channels are blocked in a voltage-dependent manner by the solutes. To best observe changes in the shape of G_{Na}-V relations that reflect the presence of voltage dependent block, each G_{Na}-V relation was normalized so that $G_{Na(max)}$ was set to 1.

Figure 4*A–H* shows G_{Na}-V relations for the test solutes at near ED_{50} concentrations for I_{Na} block (filled circles) and their Ringer's solution pre-application control (open circles) and recovery (open squares) G_{Na}-V relations. Each of the solutes caused two changes in the G_{Na}-V relations obtained in Ringer's solution; in the presence of the solute, G_{Na}-V relations shift to the right and their slope is decreased. The solute induced a depolarizing (rightward) shift in the G_{Na}-V relations to cause G_{Na} to be reduced at all voltages until G_{Na} saturates. However, since all test solute G_{Na}-V relations were normalized, solute-induced reductions in $G_{Na(max)}$ are not illustrated in Fig. 4. On average, there is a 41% reduction of $G_{Na(max)}$ upon exposure of a solute to Na^+ channels near ED_{50} doses.

$G_{Na(max)}$ in the presence of propanol, butanol, and pentanol was respectively reduced to 59, 54, and 60% control $G_{Na(max)}$. Similarly, in the presence of benzyl alcohol, phenethyl alcohol and 3-phenyl propanol, $G_{Na(max)}$ was reduced to 61, 61, and 60% control $G_{Na(max)}$, respectively. A pairwise comparison of each *n*-alkanol with its phenyl-substituted counterpart reveals that there is no significant difference in the reduction of $G_{Na(max)}$ by the addition of a phenyl group to the parent compound. The results suggest that increases in chain length do not cause any systematic reduction in $G_{Na(max)}$.

Solutes also produced changes in the slope of G_{Na}-V relations which reflect the presence of voltage dependent

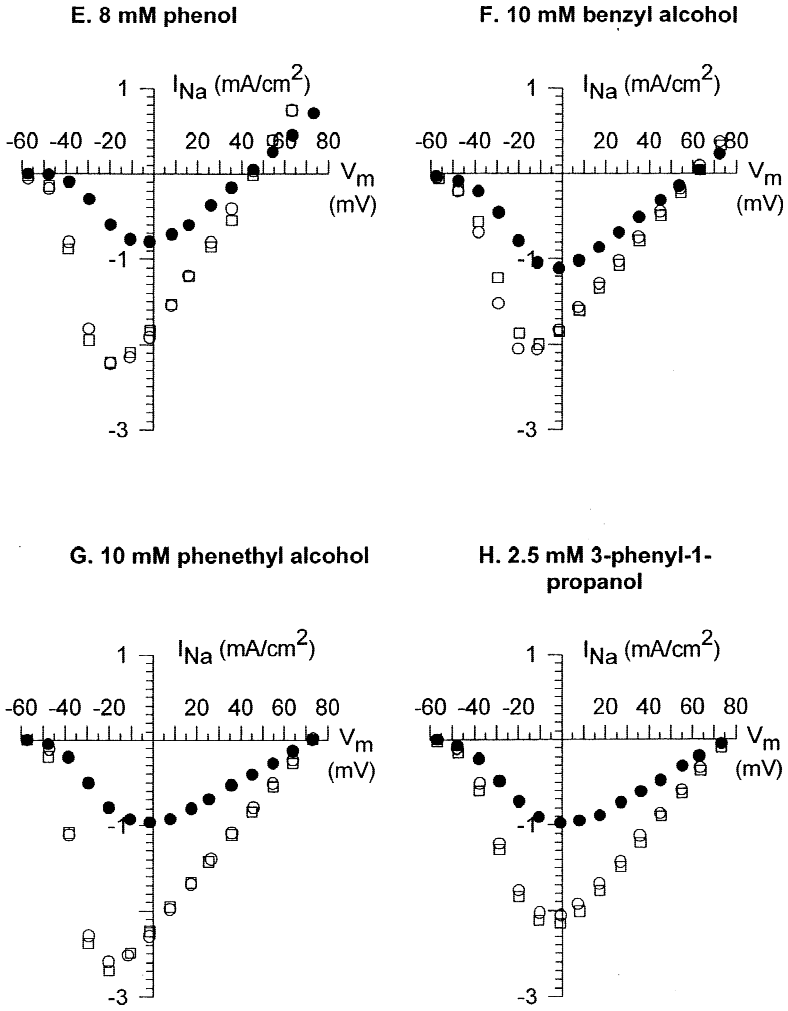

Fig. 2. (*E–H*) Na^+ current-voltage relations for (*E*) phenol, (*F*) benzyl alcohol, (*G*) phenyl alcohol, (*H*) 3-phenyl-1-propanol. For details *see* legend to Fig. 2*A–D*.

block. Table 2 compiles the results of the shift ($\Delta V_{1/2}$) and changes in slope (z) produced by the solutes at ED_{50}s for I_{Na} block. The values in the table were obtained in the following way. The mean values of $\Delta V_{1/2}$ ($\geq$3 replications) obtained for each solute were plotted for all concentrations of the solute used ($\geq$5). Plots produced linear relationships between $\Delta V_{1/2}$ and concentration; $\Delta V_{1/2}$ increased as a function of concentration. Using previously obtained ED_{50} values for I_{Na} block, the corresponding $\Delta V_{1/2}$s were calculated. A similar procedure was used to calculate values of Δz at ED_{50}s for I_{Na} block; Δz also linearly increased as a functin of concentration.

Table 2 shows that there were no systematic changes in $\Delta V_{1/2}$ and Δz for the three *n*-alkanols; the respective means for *n*-alkanols were 7.6 and −1.79. Similarly, for Φ-alkanols there were no systematic changes in $\Delta V_{1/2}$ and Δz. Phenol produced values of $\Delta V_{1/2}$ and Δz that were not much different than those obtained for Φ-alkanols. However, the mean values of $\Delta V_{1/2}$ and Δz (11.1 and −2.03, respectively) for Φ-alkanols and phenol were significantly larger that those for *n*-alkanols suggesting that the presence of a phenyl group acted to produce a greater shift in $V_{1/2}$ and a larger reduction in the slope of G_{Na}-V relations. These results are consistent with the idea that phenol and Φ-alkanols more effectively reduce G_{Na} and produce a greater voltage dependent block of Na channels.

Alkanol Size, Log K_{ow} and ED_{50}

To characterize the relationship between solute size and ED_{50}, ED_{50} was plotted *vs.* the number of carbons in the molecule. Two distinct linear relations between log ED_{50} and carbon number were obtained for *n*-alkanols and Φ-alkanols. The log ED_{50} value for phenol lies at a point where one would expect the value for *n*-hexanol to be placed on the log ED_{50} *vs.* carbon number for *n*-alkanols. However, the relation between the log ED_{50} and Φ-alkanol carbon number does not follow along the same path specified by the linear relation between log ED_{50} *vs.* carbon number for *n*-alkanols.

In both sets of alkanols the logarithm of the ED_{50} decreases linearly with an increase in the chain length of

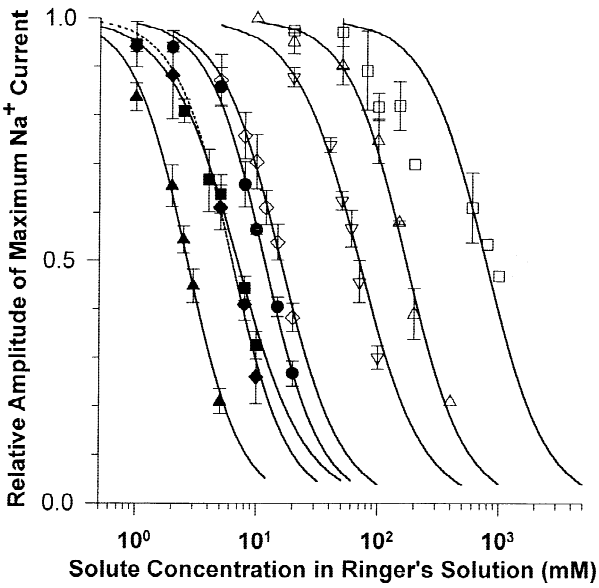

Fig. 3. Dose-response relations for I_{Na} block. Dose-response relations obtained for ethanol (open squares), *n*-propanol (open triangles), *n*-butanol (open inverted triangles), *n*-pentanol (open diamonds), phenol (filled diamonds), benzyl alcohol (filled circles), phenethyl alcohol (filled squares), and 3-phenyl-1-propanol (filled triangles). Each plotted point represents the mean relative I_{Na} ± SEM for a particular concentration of a test solute in Ringer's solution. At least three (range 3–8) replications of each concentration were used to calculate the mean. Solid traces: dose-response curves for I_{Na} block were calculated using a logistics equation (*see* text).

the molecule. However, the relations for Φ-alkanols possess reduced slopes compared to the slopes for relations for *n*-alkanols. These observations suggest that the log ED_{50} is not solely determined by the size of the molecule.

To determine whether the solute lipid solubility can solely determine I_{Na}/G_{Na} blocking potency, ED_{50}s were plotted on a logarithmic scale as a function of their log K_{ow}. No single relation between the log ED_{50} and the log K_{ow} can predict the behavior of both groups of molecules. Instead, two separate almost parallel linear relations are observed. This suggests that the log K_{ow} does not solely determine the ED_{50} or the potency.

Alkanol-Induced Changes in Steady-State Inactivation

Alkanols altered Na channel inactivation. To characterize the changes in steady-state inactivation caused by alkanols, the following protocol was used: a 50 msec prepulse was followed by a 0 mV test pulse. A sequence of prepulses from −140 to +10 mV in steps of 10 mV was used. The amplitude of I_{Na} elicited during the test pulse relative to the maximum amplitude of I_{Na} obtained using a −140 mV prepulse was plotted as a function of the prepulse potential. Solutes were applied at near ED_{50} doses. Each solute produced a reversible hyperpolarizing (leftward) shift in the h_∞ relation; thus at any given potential the test solute reduced the peak I_{Na}. The results obtained for 50 mM butanol (−8 ± 1.5 mV) and 15 mM pentanol (−9 ± 0.9 mV) were similar to the those shown by Elliott and Elliott (1991) and served as controls for the h_∞ shifts produced by Φ-alkanols.

Shifts in h_∞ for 10 mM benzyl alcohol (−13 ± 3.1 mV), 8 mM phenethyl alcohol (−13 ± 1.8 mV), and 2.5 mM 3 phenyl-1-propanol (−12 ± .5 mV) were not statistically different. The h_∞ shifts observed for Φ-alkanols were significantly larger than those observed for *n*-alkanols. Elliott and Elliott (1991) showed that *n*-alkanols caused hyperpolarizing h_∞ shifts that were independent of the size of the alkanol. Similar results were obtained using Na channels from a number of different species, including squid, frog, and rat (Elliott & Elliott, 1991). h_∞ shifts for Φ-alkanols appear to also be independent of Φ-alkanol size.

Alkanols Alter Na Channel Kinetics

To characterize any kinetic changes produced by *n*-alkanols and Φ-alkanols, Na currents were fit with a kinetic model and the solute treated currents were compared with their corresponding Ringer's solution controls. Comparisons were made over a range of voltages in order to best detect any solute induced changes in kinetics. The kinetic model chosen to make comparisons was a modified version of the Hodgkin and Huxley (1952*b*) HH model for I_{Na}. Since the HH model does not adequately describe the presence of delays in the development of activation and inactivation, they were incorporated in to the HH model to produce a modified model. Muscle I_{Na}s also display two time constants of fast inactivation (Hahin, 1988; Hahin 1990); this was also incorporated into the model. The kinetic model used was:

$$I_{Na} = I_{Na(max)} (e^{-(t-d1)/\tau m})^3 (W\, e^{-(t-d2)/\tau h-f} + (1-W)\, e^{-(t-d2)/\tau h-s}), \quad (7)$$

where I_{Na} is the observed Na current, $I_{Na(max)}$ is the maximum attainable inward Na^+ current, $d1$ is the activation delay, τ_m is the activation time constant, W is the relative amplitude of the fast component of rapid inactivation (fraction of fast inactivating Na^+ channels), $d2$ is the inactivation delay, τ_{h-f} is the fast inactivation time constant, $1 - W$ is the relative amplitude of the slow component of rapid inactivation (fraction of slowly inactivating Na^+ channels), and τ_{h-s} is the slow component inac-

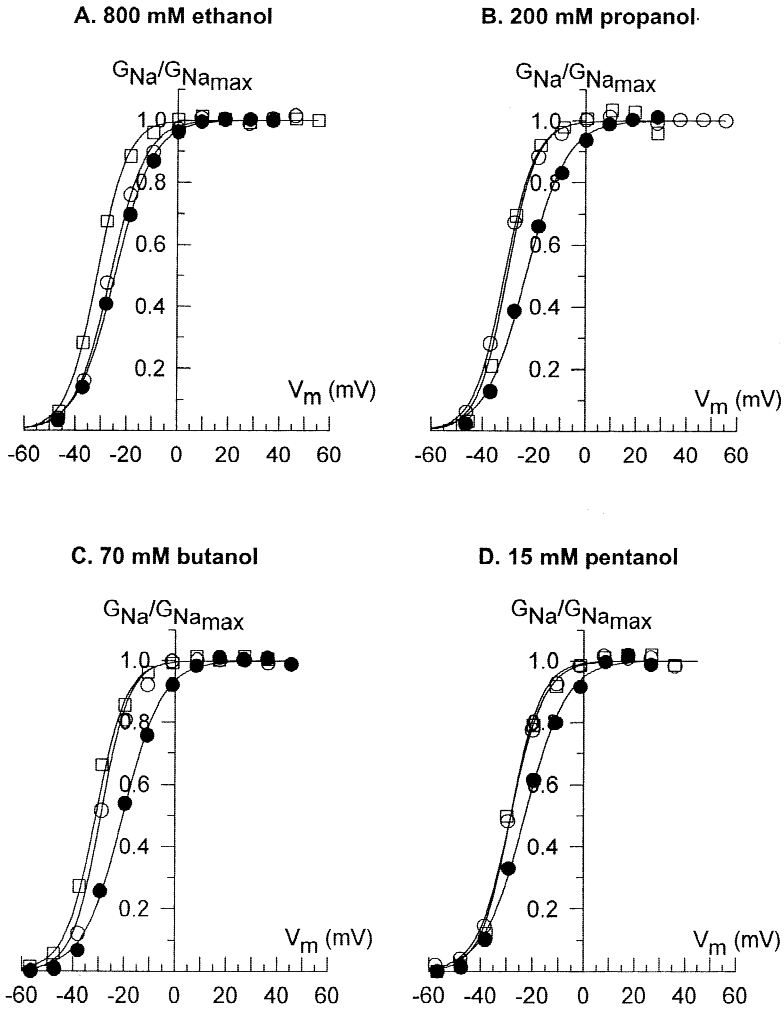

Fig. 4. (*A–D*) Normalized conductance vs voltage (G_{Na}–V) relations for alkanol solutes at near ED_{50} concentrations. Relations were obtained from fibers bathed in Ringer's solution (open circles), in the test solute at near ED_{50} concentration (filled circles; concentration indicated above the corresponding curve-set), and in Ringer's solution following washout of test solute (open squares). The points represent normalized G_{Na} plotted as a function of membrane potential (*A*) Ethanol, (*B*) *n*-propanol, (*C*) *n*-butanol, (*D*) *n*-pentanol. Each curve-set represents one experiment.

tivation time constant. The above modified HH model was chosen for use because it allowed kinetic comparisons to be made with previously published kinetic analyses of the action of *n*-alkanols made using the HH model.

Table 3 shows kinetic parameters obtained in Ringer's solution from fitting the I_{Na}s with nonlinear least squares fits to Eq. 7. Shown are the activation time constant (τ_m), two fast inactivation time constants (τ_{h-f} and τ_{h-s}), two relative amplitudes of fast inactivation, where W represents the relative amplitude of the rapid component of fast inactivation and $1 - W$ represents the relative amplitude of the slow component of fast inactivation, and the delays for the activation ($d1$) and fast inactivation ($d2$). In order to insure adequate comparisons between voltage-shifted kinetic parameters obtained in the test solute relative to the kinetic parameters obtained in Ringer's solution, the following procedure was employed: kinetic parameter comparisons were made only after compensating for the voltage dependent shifts in G_{Na}-V relations observed for each test solute.

Table 2. Voltage-dependent shifts of G_{Na}-V Relations at ED_{50}s

Solute	$\Delta V_{1/2}$ mV	$-\Delta z$ mSiemens cm^{-2} mV^{-1}
n-Alkanols		
n-Propanol	8.1 ± 0.71	1.47 ± 0.13
n-Butanol	5.4 ± 0.21	1.48 ± 0.06
n-Pentanol	9.4 ± 0.71	2.41 ± 0.18
Mean ± SEM	7.6 ± 1.2	1.79 ± 0.31
Phenol and Φ-Alkanols		
Phenol	14.4 ± 0.52	2.16 ± 0.08
Benzyl alcohol	12.3 ± 0.67	1.98 ± 0.11
Phenethyl alcohol	9.51 ± 0.40	2.03 ± 0.09
3-Phenyl-1-propanol	11.6 ± 0.23	2.08 ± 0.04
Mean ± SEM (excluding phenol)	11.1 ± 0.80	2.03 ± 0.03

$\Delta V_{1/2}$–depolarizing shift at the midpoint of G_{Na}-V relations.
Δz–change of the slope at the mid-point of G_{Na}-V relations.

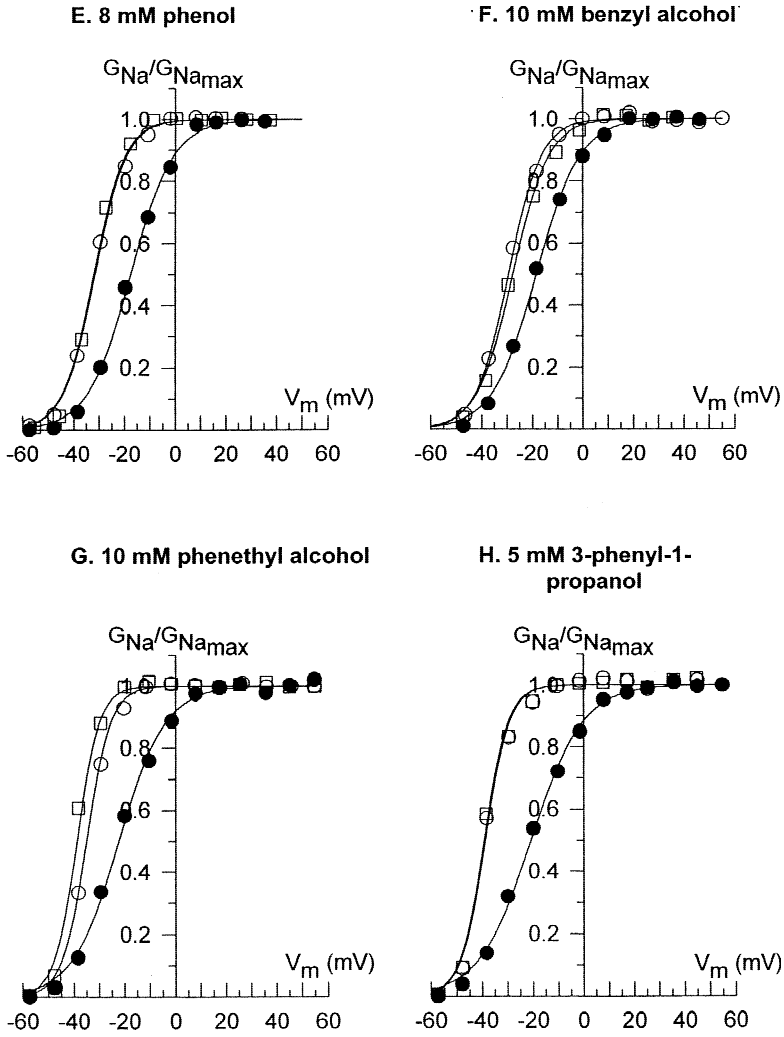

Fig. 4. (*E–H*) Normalized conductance vs voltage (G_{Na}-V) relations for alkanol solutes at near ED_{50} concentrations. (*E*) Phenol, (*F*) benzyl alcohol, (*G*) phenethyl alcohol, and (*H*) 3-phenyl-1-propanol. For details, *see* legend to Fig. 2*A–D*.

Table 4*A–C* shows the significantly affected I_{Na} kinetic parameters reported as a ratio relative to their values in Ringer's solution. Table 4*A–C* also shows the difference between the parameters (d_j) obtained in the presence of the solute compared to Ringer's solution and the minimum detectable difference (δ) for significance for the sample size. All concentrations used were near ED_{50} values.

Since there were no systematic changes in the relative ratio of parameters as the size of the molecule increased, a mean ratio could be obtained for each parameter for *n*-alkanols and Φ-alkanols. $\tau_{m(S)}/\tau_{m(R)} = 0.77 \pm 0.05$ (*n*-alkanols) and 0.76 ± 0.04 (Φ-alkanols), while $\tau_{h-f(S)}/\tau_{h-f(R)} = 0.60 \pm 0.06$ (*n*-alkanols) and 0.52 ± 0.03 (Φ-alkanols). Similarly $d2_{(S)}/d2_{(R)} = 0.73 \pm 0.04$ (*n*-alkanols) and 0.70 ± 0.03 (Φ-alkanols). The differences between *n*- and Φ-alkanols and phenol were not significant. Thus, both *n*-alkanols and Φ-alkanols and phenol caused τ_m to be reduced to 76% of its original value observed in Ringer's solution. Similarly, τ_{h-f} and $d2$ were reduced to 55 and 71%, respectively, by both *n*-alkanols and Φ-alkanols and phenol.

Discussion

Comparison of Results

Alkanol-Induced Block of I_{Na}

Two studies (Armstrong & Binstock, 1964; Haydon & Urban, 1983) showed that alkanols block I_{Na}s in squid giant axons. Elliott and Haydon (1989) reported an ED_{50} (14.8 [7]) for I_{Na} block by *n*-pentanol and benzyl alcohol (12[2]) that does not significantly differ from the corresponding ED_{50}s (16 ± 0.8 and 11.7 ± 0.3) for I_{Na} block obtained in this study. Also in this study, ED_{50} for I_{Na} block declined (and the relative potencies increased) by 3.6 ± 0.8 for the addition of each methylene group from methanol to *n*-pentanol compared to a previously reported value of 3.7 ± 0.2 (Elliott & Haydon, 1989).

Table 3. Na current kinetic parameters obtained in Ringer's solution

V_m, mV	−11	−1	8	18	27
τ_m, msec	0.219 ± 0.008	0.183 ± 0.005	0.160 ± 0.004	0.143 ± 0.003	0.129 ± 0.003
$\tau_{h\text{-}f}$, msec	0.686 ± 0.024	0.625 ± 0.020	0.566 ± 0.019	0.524 ± 0.018	0.495 ± 0.018
$\tau_{h\text{-}s}$, msec	3.57 ± 0.417	5.22 ± 0.586	6.88 ± 0.805	7.76 ± 1.47	7.88 ± 1.56
W	0.912 ± 0.011	0.957 ± 0.006	0.968 ± 0.005	0.970 ± 0.008	0.958 ± 0.015
*d*1, msec	0.093 ± 0.003	0.079 ± 0.003	0.070 ± 0.003	0.069 ± 0.004	0.064 ± 0.003
*d*2, msec	0.709 ± 0.012	0.643 ± 0.010	0.586 ± 0.009	0.536 ± 0.008	0.476 ± 0.012

V_m–membrane potential,
τ_m–activation time constant,
$\tau_{h\text{-}f}$–fast inactivation time constant,
$\tau_{h\text{-}s}$–slow inactivation time constant,
W–fraction of rapidly inactivating Na^+ channels,
*d*1–activation delay,
*d*2–inactivation delay.

Alkanols Alter Kinetics of I_{Na}

Elliott and Haydon (1989) reviewed previous studies that examined the effect of *n*-pentanol and benzyl alcohol on the kinetics of I_{Na}. Their analysis of I_{Na} kinetics at ED_{50}s for I_{Na} block revealed that *n*-pentanol and benzyl alcohol did not reduce the maximum possible conductance ($\bar{g}_{Na}$) and produced only small depolarizing shifts in steady-state inactivation (h_∞ relations), seemingly contradictory to the results obtained in the present study. Also *n*-pentanol and benzyl alcohol produced large depolarizing shifts in steady-state activation (m_∞ curves) and reduced I_{Na} time constants of activation (τ_m) and inactivation (τ_h).

The results of Elliott and Haydon (1989) and a study conducted by Armstrong and Binstock (1964), which showed that *n*-propanol decreased G_{Na}, are compared with the results of this study in Table 5. Relative values of peak I_{Na} ($I_{Na(Solute)}/I_{Na(Ringer)}$), maximum G_{Na} ($G_{Na(S)}/G_{Na(R)}$) calculated in this study, and $\bar{g}_{Na}$ ($\bar{g}_{Na(S)}/\bar{g}_{Na(R)}$) calculated by Elliott and Haydon (1989), shifts in the midpoint of the steady-state activation ($\Delta V_m(m_\infty)$), G_{Na}-V relations ($\Delta V(G_{Na}$-$V)$), and steady-state inactivation ($\Delta V(h_\infty)$), and the relative amplitudes of the activation time constant ($\tau_{m(S)}/\tau_{m(R)}$) and inactivation time constant ($\tau_{h(S)}/\tau_{h(R)}$) are tabulated.

The kinetic analysis of HH parameters of I_{Na} performed by Elliott and Haydon (1989) differed from the analysis used in this study since maximum G_{Na}s were different. In the Elliott and Haydon (1989) analysis, $\bar{g}_{Na}$ represents a constant independent of voltage (Hodgkin & Huxley, 1952*a*) that is related to maximum G_{Na} by the relation: $G_{Na(max)} = \bar{g}_{Na}\, m_\infty^3$ when the initial value of the activation variable $m_0 = 0$. The shifts of m_∞ are reported in Table 5 as $\Delta V_m(m_\infty)$. In the present study, the maximum G_{Na}-V was obtained from Eq. 3; the shifts of G_{Na}-V are reported in Table 5 as $\Delta V(G_{Na})$. To overcome the differences in concentrations used in the studies, Eq. 1, 2, and 3 were used to calculate the $G_{Na(max)}$ obtained by Elliott and Haydon (1989) for *n*-pentanol and benzyl alcohol at the same concentrations. The calculated values are reported in [brackets] in Table 5.

Elliott and Haydon (1989) reported large depolarizing shifts in the steady-state activation parameter m_∞ ($\Delta V_m(m_\infty)$ in Table 5). The m_∞ shifts are related to the depolarizing shifts experimentally observed in G_{Na}-V relations, since $G_{Na(max)} = \bar{g}_{Na}\, m_\infty^3$ when m_0 is negligible. The m_∞ curve was shifted by 16 and 10 mV by 14.8 mM *n*-pentanol and 12 mM benzyl alcohol, respectively. The calculated values of relative $G_{Na(max)}$ for 14.8 mM *n*-pentanol and 12 mM benzyl alcohol were 0.58 and 0.61, respectively. Using the squid m_∞ curve (Hodgkin & Huxley, 1952*b*) and the reported shifts, the estimated values for m_∞ were 0.6 for *n*-pentanol and 0.68 for benzyl alcohol. Since $\bar{g}_{Na}$ reported by Elliott and Haydon (1989) was reduced to 0.96 by *n*-pentanol and to 0.92 by benzyl alcohol, the calculated values for relative $G_{Na(max)}$ were 0.58 for *n*-pentanol and 0.62 for benzyl alcohol, which are nearly identical to the corresponding values (reported in ⟨brackets⟩) for this study. Thus, the shift of G_{Na}-V relations ($\Delta V(G_{Na})$) reported in this study appears as a corresponding shift of m_∞ reported by Elliott and Haydon (1989) and fit well with that study.

Time constants of activation and inactivation were reduced by *n*-alkanols and benzyl alcohol in both studies. Elliott and Haydon (1989) reported values for *n*-pentanol and benzyl alcohol only; their review of the results obtained in other studies suggested that all *n*-alkanols reduced τ_m and τ_h, similar to the results obtained in this study.

Armstrong and Binstock (1964) examined the effect of *n*-propanol on maximum G_{Na} and changes in h_∞; their results are compared with the results of this study. To better perform the comparison, $G_{Na(S)}/G_{Na(R)}$ for *n*-

Table 4. Test solutes alteration of I_{Na} kinetic parameters

Solute	C, mM	$\tau_{m(Solute)}/\tau_{m(Ringer)}$	d_j, *msec*	δ, msec
Activation time constant (τ_m)				
Ethanol	800	0.623 ± 0.023	0.081 ± 0.016*	0.065
Propanol	150	0.835 ± 0.047	0.028 ± 0.008*	0.026
Butanol	70	0.796 ± 0.045	0.043 ± 0.012*	0.040
Pentanol	15	0.806 ± 0.021	0.037 ± 0.006*	0.014
Phenol	5	0.772 ± 0.023	0.041 ± 0.005*	0.017
	8	0.660 ± 0.024	0.058 ± 0.008*	0.024
Benzyl alcohol	10	0.763 ± 0.021	0.043 ± 0.006*	0.017
Phenethyl alcohol	5	0.676 ± 0.037	0.052 ± 0.009*	0.028
	8	0.826 ± 0.034	0.030 ± 0.008*	0.024
3-Phenyl-1-propanol	2.5	0.884 ± 0.021	0.019 ± 0.004*	0.011
Fast Component of inactivation time constant ($\tau_{h\text{-}f}$)				
Solute	C, mM	$\tau_{h\text{-}f(S)}/\tau_{h\text{-}f(R)}$	d_j, msec	δ, msec
Ethanol	800	0.592 ± 0.005	0.266 ± 0.004*	0.014
Propanol	150	0.759 ± 0.093	0.270 ± 0.099*	0.113
Butanol	70	0.495 ± 0.024	0.310 ± 0.017*	0.057
Pentanol	15	0.552 ± 0.014	0.287 ± 0.012*	0.039
Phenol	5	0.501 ± 0.007	0.292 ± 0.012*	0.036
	8	0.394 ± 0.009	0.343 ± 0.011*	0.033
Benzyl alcohol	10	0.591 ± 0.018	0.229 ± 0.016*	0.047
Phenethyl alcohol	5	0.544 ± 0.010	0.244 ± 0.012*	0.038
	8	0.497 ± 0.019	0.349 ± 0.015*	0.046
3-Phenyl-1-propanol	2.5	0.594 ± 0.036	0.306 ± 0.039*	0.119
Inactivation delay (*d2*)				
Solute	C, mM	$d2_{(S)}/d2_{(R)}$	d_j, msec	δ, msec
Ethanol	800	0.696 ± 0.018	0.213 ± 0.015*	0.060
Propanol	150	0.819 ± 0.06	0.102 ± 0.034*	0.114
Butanol	70	0.651 ± 0.008	0.227 ± 0.009*	0.031
Pentanol	15	0.749 ± 0.021	0.156 ± 0.011*	0.037
Phenol	5	0.719 ± 0.022	0.170 ± 0.015*	0.045
	8	0.600 ± 0.014	0.235 ± 0.016*	0.048
Benzyl alcohol	10	0.728 ± 0.018	0.160 ± 0.012*	0.037
Phenethyl alcohol	5	0.642 ± 0.029	0.206 ± 0.024*	0.079
	8	0.719 ± 0.024	0.169 ± 0.014*	0.045
3-Phenyl-1-propanol	2.5	0.803 ± 0.017	0.117 ± 0.011*	0.032

C represents the solute concentration for which kinetic parameters were obtained.
d_j represents the absolute value of the mean sample difference for each parameter ± standard error of the mean (SEM)
δ represents the minimum detectable difference obtained from the following equation for a one-sample *t* test for a sample difference, d_j.

$$\delta = \sqrt{\frac{s_d^2}{n}}\,(t_{\alpha,\nu} + t_{\beta(1),\nu}),$$

where s_d^2 is a sample d_j variance, *n* is a number of observations, $t_{\alpha,\nu}$ is the probability of detecting the difference with the significance level α of 0.05, and $t_{\beta(1),\nu}$ is the probability of detecting the difference between the test and the control 90% of the time (Zar, 1996).
* indicates significant differences.

propanol was calculated from Eqs. 1, 2, and 3 used to fit G_{Na}-*V* relations in this study. The calculated values were 0.65 and 0.46 for 130 and 260 mM *n*-propanol, respectively, and are shown in ⟨brackets⟩. $G_{Na(S)}/G_{Na(R)}$ for *n*-propanol fits fairly well with the corresponding values obtained by Armstrong and Binstock (1964). G_{Na}-*V* shifts reported by Armstrong and Binstock (1964) produced by *n*-alkanols were similar in size to shifts reported in this study for ED_{50}s (Δ*V*) in Table 2).

A discrepancy was seen when comparing shifts in h_∞. In this study hyperpolarizing shifts of 9 and 13 mV were observed for *n*-pentanol and benzyl alcohol, respectively. Armstrong and Binstock (1964) reported no shifts in h_∞ by *n*-alkanols, whereas Elliott and Haydon

Table 5. Kinetic parameters of I_{Na} from three separate studies

Study	Solute	Test conc. (mM)	Rel. max G_{Na}	Rel. $\bar{g}_{Na}$	ΔV_m (m_∞) (mV)	ΔV (G_{Na}) (mV)	ΔV (h_∞) (mV)	Rel. τ_m	Rel. τ_h
Armstrong & Binstock (1964)	*n*-Propanol	130 (2)	0.64			≈5	0		
		260 (1)	0.61				0		
Elliott & Haydon (1989)	*n*-Pentanol	14.8 (3)	[0.58]	0.96	16		2.8	0.57	0.71
	Benzyl alcohol	12 (2)	[0.62]	0.92	10.1		−3.4	0.68	0.58
Present study	*n*-Propanol	100 (4)				5.8			
		150 (3)				6.7		0.84	0.76
	n-Pentanol	12 (3)	0.68			6	−9		
		15 (6)	0.62			7.3		0.81	0.55
	Benzyl alcohol	10 (6)	0.69			8.3	−13	0.76	0.59
		15 (3)	0.52			11			
Present study	*n*-propanol	130	<0.65>						
(calculated values)		260	<0.46>						
	n-pentanol	14.8	<0.58>						
	Benzyl alcohol	12	<0.61>						

Rel. I_{Na} is the relative amplitude of peak Na current.
Rel. $G_{Na(max)}$ is the relative maximum Na conductance ($G_{Na(max)}$) obtained in the present study.
Rel. $\bar{g}_{N\text{-}a}$ is the relative maximum possible Na conductance ($\bar{g}_{Na}$) obtained by Elliott and Haydon (1989).
$\Delta V_m(m_\infty)$ is the shift in the mid-point of the steady-state activation (m_∞) curve.
$\Delta V(G_{Na})$ is the shift in the mid-point of the G_{Na}-V curve.
$\Delta V(h_\infty)$ is the shift in the mid-point of the steady-state inactivation (h_∞) curve.
Rel. τ_m is the relative time constant of activation.
Rel. τ_h is the relative time constant of inactivation.
Armstrong & Binstock (1964) and Elliott & Haydon (1989) used squid giant axons.
Numbers in parentheses give the number of observations.

(1989) observed a 2.8 mV depolarizing shift produced by *n*-pentanol and a 3.4 mV hyperpolarizing shift produced by benzyl alcohol. The present study shows that the test solutes inactivated more frog Na channels than that shown previously for squid Na channels. However, *n*-butanol and *n*-pentanol were shown to produce hyperpolarizing shifts of h_∞ of −11 mV in rat dorsal root ganglia (Elliott & Elliott, 1991), similar to the shifts obtained in this study.

The differences between h_∞ may have resulted from two likely sources. (i) Armstrong & Binstock (1964) and Elliott and Haydon (1989) used squid giant axons which were immersed in artificial sea water; the ionic strength of artificial sea water is much greater than the ionic strength of Ringer's solution used in the present study. The greater ionic strength of artificial sea water may decrease the octanol-water partition coefficients of polar alkanols and thus reduce the efficacy of alkanols to alter inactivation. (ii) Alkanol-induced h_∞ shifts may depend on species-specific properties of Na channels.

Alkanol-Induced Block of K^+ Currents

Previous studies have shown that *n*-alkanols suppressed Na^+ currents more than they suppressed K^+ currents (Armstrong & Binstock, 1964; Haydon & Urban, 1986; Elliott & Haydon, 1989). Haydon and Urban (1986) reported that the concentrations of *n*-alkanols required to suppress 50% of I_{Na}, were 2–9 times smaller than the concentrations of *n*-alkanols required to suppress 50% of I_K. Armstrong and Binstock (1964) reported that alkanols suppressed maximum G_K less than maximum G_{Na}, similar to the anesthetic procaine. These results suggest that alkanols act by primarily altering Na^+ channels.

Phenyl Substitution Changes Physical-Chemical Properties of n-Alkanols and Increased Their Anesthetic Potency

Table 6 shows the ED_{50}s for AP block and I_{Na} block obtained for each of the solutes along with their physical-chemical properties: intrinsic molar volume (V_i), polarity (P), and hydrogen bond acceptor basicity (β) and donor acidity (α), which are tabulated in columns. P, β, and α were derived from the work of Taft et al. (1985) and Kamlet et al. (1988); P represents a scalar measure of the high frequency polarizability of the solute while β and α provide a measure of the ability of the solute to accept or donate a hydrogen bond, respectively.

The intrinsic molar volume, which represents a measure of molecular size, increases by approximately 10 ml/M with each additional methylene group added to an *n*-alkanol. Addition of a phenyl group to an *n*-alkanol increased the size of the molecule by 43 ml/M. Thus phenyl group substitution substantially increased the size

Table 6. Experimentally obtained ED_{50}s and Physical-chemical properties of solutes

Solute	ED_{50} (mM)			Physico-chemical properties			
	AP Block	I_{Na} Block	$V_l/100$	P	β	α	log K_{ow}
n-Alkanols							
Methanol	2392 ± 54		0.205	0.40	0.42	0.35	−0.77
Ethanol	881 ± 30	779 ± 19	0.305	0.40	0.45	0.33	−0.31
n-Propanol	235 ± 8	171 ± 11	0.405	0.40	0.45	0.33	0.25
n-Butanol	69 ± 3	70 ± 3	0.499	0.40	0.45	0.33	0.88
n-Pentanol	20 ± 1	16 ± 0.8	0.593	0.40	0.45	0.33	1.56
n-Hexanol	7.0 ± 0.6		0.690	0.40	0.45	0.33	2.03
n-Heptanol	2.3 ± 0.1		0.788	0.40	0.45	0.33	2.72
Phenol and M-alkanols							
Phenol	8.1 ± 0.3	6.3 ± 0.4	0.536	0.72	0.33	0.61	1.46
Benzyl alcohol	20 ± 0.5	11.7 ± 0.3	0.634	0.99	0.52	0.39	1.10
Phenethyl alcohol	10 ± 0.6	6.7 ± 0.4	0.732	0.97	0.55	0.33	1.51
3-Phenyl-1-propanol	3.1 ± 0.2	2.0 ± 0.1	0.830	0.95	0.55	0.33	2.05

ED_{50}–solute concentration producing 50% block.
$V_l/100$–intrinsic molar volume/100 (ml/M × 10^{-2}).
P–polarity (high frequency polarizability).
β–hydrogen bond acceptor basicity.
α–hydrogen bond donor acidity.
log K_{ow}–octanol-water partition coefficient.

of each *n*-alkanol; the percent increase in size due to phenyl substitution decreases as the size of the parent *n*-alkanol increases. Thus, benzyl alcohol is more than 3 times the size of methanol while 3-phenyl-l-propanol is only slightly more than 2 times the size of *n*-propanol.

The polarity of unsubstituted *n*-alkanols does not change with the addition of methylene groups, whereas the polarity of phenyl substituted *n*-alkanols decrease upon addition of methylene groups. The ability to accept (β) or donate (α) a hydrogen bond does not change as the size of an *n*-alkanol increases. Unsubstituted *n*-alkanols are better acceptors of hydrogen bonds than donors. However, phenyl substituted *n*-alkanols accept hydrogen bonds better than unsubstituted *n*-alkanols. The ability of an *n*-alkanol to donate a hydrogen bond changes little with phenyl substitution.

The ED_{50} values decreased as the octanol-water partition coefficients (K_{ow}) and the size (V_l) of the molecule increased. Since *P* and β changed little or not at all from one alkanol to another, molecular size is a key determinant of ED_{50}, relative potency, and K_{ow}. Each additional methylene group increased the size, K_{ow}, and the potency of the *n*-alkanols. Thus each additional methylene group made each successive *n*-alkanol more hydrophobic. Phenyl group addition to *n*-alkanols increases their lipid solubility; the K_{ow} of each of the three Φ-alkanols is at least 60 times as great as its unsubstituted counterpart. An *n*-alkanol of comparable size to a Φ-alkanol is the more potent and hydrophobic of the two molecules.

Adding a phenyl group to an *n*-alkanol increases the solute's size, polarity, the ability to accept H-bonds, and its lipid solubility. Thus Φ-alkanols are less hydrophobic than unsubstituted *n*-alkanols of similar size. Phenol and phenyl substituted *n*-alkanols are polar anesthetics. Phenol accepts hydrogen bonds less than and donates hydrogen bonds better than all test *n*-alkanols. Although its size and K_{ow} are smaller than the size and K_{ow} of *n*-pentanol, phenol ($ED_{50(AP\ block)}$ = 8.1 mM) is more potent than *n*-pentanol (ED_{50} = 20 mM). Thus the potency is not solely determined by size and/or K_{ow}.

The chain length and K_{ow} were found to be important factors in determining the potency of alkanols. However, neither the chain length nor log K_{ow} solely determined blocking potency. The potency of I_{Na} block in a homologous series of *n*-alkanols increased by 3.6 ± 0.8 for every methylene group added. The potency increase per methylene group for phenyl substituted *n*-alkanols was not constant, but instead increased as the methylene chain increased. Phenyl-substituted ethanol (phenethyl alcohol) was two times more potent than phenyl-substituted methanol (benzyl alcohol), whereas phenyl-substituted *n*-propanol (3-phenyl-1-propanol) was more than three times more potent than phenethyl alcohol. The potency increase per methylene group is likely to converge to 3.2 (potency increase per methylene group for *n*-alkanols) as the Φ-alkanol is extended in size. Phenyl substitution increased the potencies of corresponding *n*-alkanols. Phenyl group addition to an *n*-alkanol simply increases the potency independent of the chain length of the *n*-alkanol (up to 3-carbon chain).

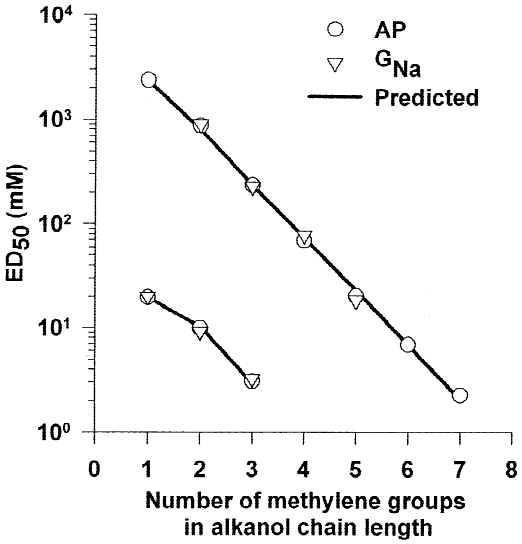

Fig. 5. Predictions of ED_{50}'s for *AP* and G_{Na} block for alkanols. ED_{50}'s for *AP* (circles) and G_{Na} (triangles) block for *n*-alkanols and Φ-alkanols as a function of the number of methylene groups in the solute. Predictions for ED_{50}'s for G_{Na} block based on equation 8 are shown as solid traces.

Predictions of ED_{50}

Using multiple linear regression analysis an equation designed to predict ED_{50} G_{Na} block as a function of the physical chemical properties of the solutes was derived:

$$ED_{50} = 10^{(-5.36\, V_I + 0.88\, P - 1.06\, \beta - 4.92\, \alpha + 6.29)}, \quad (8)$$

where V_l is the solute intrinsic molar volume, β is the hydrogen bond acceptor basicity, α is the hydrogen bond donor acidity, and P is the polarity of the solute.

Figure 5 shows ED_{50}s for AP (circles) and G_{Na} (triangles) block for *n*-alkanols and Φ-alkanols as a function of the number of methylene groups in the solute. Superimposed on the symbols are predictions of ED_{50}s for G_{Na} block based on Eq. 8; the traces represent predictions for both, *n*-alkanols and Φ-alkanols. The predictions are quite good. The equation adequately predicts ED_{50}s for both G_{Na} and AP block. These results suggest that variations in ED_{50} can be adequately explained as a function of V_i, P, β, and α.

Equation 8 also predicts ED_{50}s of *n*-alkanols and Φ-alkanols and phenol for AP block. This observation was unexpected, since Na channel block is nonlinearly related to AP block. A 50% block of Na channels typically results only in a small (less than 10%) reduction in AP size. However, Na channel block in itself does not simply explain AP block. Other changes in Na channel properties produced an additional apparent block of Na channels. These changes include depolarizing shifts in G_{Na}-V relations, changes in Na current kinetics, and hyperpolarizing shifts in h_∞. The contribution of each of these changes are briefly discussed below.

Voltage-Dependent Block of Na^+ Channels

All test solutes acted to produce a voltage-dependent block of I_{Na}; the reduction in I_{Na} increased with increases in membrane potential. At near ED_{50} concentrations unsubstituted and phenyl-substituted *n*-alkanols significantly decreased the slope (z) of G_{Na}-V relations (Table 3) at their midpoint; the mean reduction in slope was 1.9 ± 0.2 mSiemens cm^{-2} mV^{-1}. In addition to the voltage-dependent block of Na channels, there was a larger voltage-independent block of the channels.

Alkanols Accelerate Kinetics of I_{Na}

At nearly half-blocking doses, alkanols sped up I_{Na} activation by 24% and almost doubled the rate of fast inactivation. I_{Na} inactivation also occurred 29% earlier than normally oberved in Ringer's solution. These kinetic effects act to reduce the peak I_{Na} at any voltage.

The effect of reductions in time constants τ_m and τ_{h-f}, and inactivation delay ($d2$) produced a small effect (<5% decrease) on the peak I_{Na}. I_{Na} peaks and then inactivates faster than normal in the presence of an alkanol. However, at nearly ED_{50} alkanol concentrations, kinetic changes via simulations produced an estimated 17% reduction in the AP height.

Similar to fluidizing agents which speed up the kinetics of I_{Na} by decreasing the values of τ_m and τ_h (Elliott & Haydon, 1989), alkanols and phenol accelerated the kinetics of I_{Na}. However, alkanols caused kinetic changes that have only a nominal effect on the amplitude of I_{Na} thus the Na^+ channel blocking effect cannot be simply attributed to membrane fluidity increases.

Alkanols Inactivate Na^+ Channels

Phenyl substituted *n*-alkanols acted to significantly increase the number of inactivated Na^+ channels at the resting potential. At near ED_{50} concentrations unsubstituted *n*-alkanols shifted h_∞ relations at the midpoint by −8.7 mV and increased the slope at the midpoint of h_∞ curves, whereas phenyl substituted *n*-alkanols produced −12.5 mV shifts and comparably increased the slope of h_∞ curves. The alkanol-induced changes in the h_∞ are sufficient to cause a 28% (*n*-alkanols) and 40% (Φ-alkanols) increase in the number of inactivated Na channels for a fiber held at −80 mV.

Explanation of AP Block

Since experimentally observed and calculated ED_{50}s of *n*-alkanols for AP block are not significantly different from ED_{50}s for I_{Na} block, *n*-alkanol-induced AP block

cannot be simply explained by the block of Na^+ channels. Unsubstituted and phenyl–substituted *n*-alkanols produce AP block through a combination of effects. AP simulations based on Hodgkin-Huxley equations for squid axons (Hodgkin & Huxley, 1952*b*) were employed to estimate the percentage reduction of AP height attributed to each factor: (i) Alkanols shifted h_∞ relations in the hyperpolarizing direction and inactivated resting Na^+ channels: 22% of the AP height was reduced due to the inactivation of Na^+ channels at −80 mV by *n*-alkanols; whereas 30% of AP height was reduced due to inactivation of Na^+ channels by phenyl substituted *n*-alkanols. (ii) Alkanols equally accelerated I_{Na} kinetics which caused a 17% decrease in the AP height. (iii) Alkanols produced a voltage-independent and a voltage-dependent block of Na^+ channels and shifted G_{Na}-V relations in depolarizing direction. The composite effect of channel block and a depolarizing shift by unsubstituted and phenyl-substituted *n*-alkanols resulted in an 11 and 28% block of AP height, respectively. The combined effect of Na^+ channel inactivation, acceleration of I_{Na} kinetics, block of Na^+ channels, and depolarizing shift of G_{Na}-V relations produced an estimated 53% AP block at 50% I_{Na} blocking concentrations of unsubstituted *n*-alkanols and an estimated 75% AP block at 50% I_{Na} blocking concentrations of phenyl-substituted *n*-alkanols.

In conclusion, the results of the present study are consistent with the hypothesis that alkanol-induced AP block results from the alteration of Na^+ channels. Unsubstituted and phenyl-substituted *n*-alkanols partition into the bilayer and act on Na^+ channels by altering the Na^+ conductance and gating properties of Na^+ channels. Most importantly, they alter the inactivation of Na^+ channels. Kuroda et al. (1996) showed that the phenyl group of the local anesthetic dibucaine interacts with residues involved in Na^+ channel inactivation. Since phenyl substituted *n*-alkanols inactivated more Na^+ channels than their unsubstituted counterparts, it appears that phenyl-substitution increases the likelihood that phenyl substituted *n*-alkanols bind to Na^+ channels so as to inactivate more channels.

References

Armstrong, C.M., Binstock, L. 1964. The effects of several alcohols on the properties of the squid giant axon. *J. Gen. Physiol.* **48:**265–277

Campbell, D.T., Hahin, R. 1983. Simple shifts in the voltage dependence of sodium channel gating caused by divalent cations. *J. Gen. Physiol.* **92:**331–335

Elliott, J.R., Elliott, A.A. 1991. Action of alcohols on sodium channels in dorsal root ganglia. *Ann. New York Acad. Sci.* **625:**344–354

Elliott, J.R., Haydon, D.A. 1989. The action of neutral anaesthetics on ion conductances of nerve membranes. *Biochim. Biophys. Acta* **988:**257–286

el Tayer, N., Tsai, R.S., Tests, B., Carrupt, P.A., Leo, A. 1991. Partitioning of solutes in different solvent systems: the contribution of hydrogen-bonding capacity and polarity. *J. Pharm. Sci.* **80:**590–598

Hahin, R. 1988. Two open states or two different Na channels in skeletal muscle fibers: Markov models of the decay of Na current in frog skeletal muscle. *J. Biol. Phys.* **16:**81–91

Hahin, R. 1990. Kinetic evidence for two Na channels in frog skeletal muscle. *J. Biol. Phys.* **17:**193–211

Haydon, D.A., Urban, B.W. 1983. The action of alcohols and other non-ionic surface active substances on the sodium current of the squid giant axon. *J. Physiol.* **341:**411–427

Haydon, D.A., Urban, B.W. 1986. The action of some general anaesthetics on the potassium current of the squid giant axon. *J. Physiol.* **373:**311–327

Hille, B., Campbell, D.T. 1976. An improved Vaseline gap voltage clamp for skeletal muscle fibers. *J. Gen. Physiol.* **67:**265–293

Hodgkin, A.L., Huxley, A.F. 1952*a*. The dual effect of membrane potential on sodium conductance in the giant axon of *Loligo*. *J. Physiol.* **116:**497–506

Hodgkin, A.L., Huxley, A.F. 1952*b*. A quantitative description of membrane current and its applications to conduction and excitation in nerve. *J. Physiol.* **117:**500–544

Kamlet, M.J., Doherty, R.M., Abraham, M.H., Marcus, Y., Taft, R. 1988. Linear solvation energy relationships. 46. An improved equation for correlation and prediction of octanol/water partition coefficients of organic nonelectrolytes (including strong hydrogen bond donor solutes). *J. Phys. Chem.* **92:**5244–5255

Kuroda, Y., Ogawa, M., Nasu, H., Terashima, M., Kasahara, M., Kiyama, Y., Wakita, M., Fujiwara, Y., Fujii, N., Nakagawa, T. 1996. Locations of local anesthetic dibucaine in model membranes and the interaction between dibucaine and a Na^+ channel inactivation gate peptide as studied by ′H- and H-NMR spectroscopies. *Biophys. J.* **71:**1191–1207

Larsen, J., Gasser, K., Hahin, R. 1996. An analysis of dimethylsulfoxide-induced action potential block: A comparative study of DMSO and other aliphatic water soluble solutes. *Tox. Appl. Pharmacol.* **140:**296–314

Leahy, D.E. 1986. Intrinsic molar volume as a measure of the cavity term in linear solvation energy relationships: octanol-water partition coefficients and aqueous solubilities. *J. Pharm. Sci.* **75:**629–836

Taft, R.W., Abraham, M.H., Famini, G.R., Doherty, R.M., Abboud, J-L.M, Kamlet, M.J. 1985. Solubility properties of polymers and biological media 5: An analysis of physiochemical properties which influence octanol-water partition coefficients of aliphatic and aromatic solutes. *J. Pharm. Sci.* **74:**807–814